Characterization of cytochrome P450 CYP109E1 from Bacillus megaterium as a novel vitamin D3 hydroxylase

Abdulmughni, Ammar; Jozwik, Ilona K.; Putkaradze, Natalia; Brill, Elisa; Zapp, Josef; Thunnissen, Andy-Mark W H; Hannemann, Frank; Bernhardt, Rita

Published in:
Journal of Biotechnology

DOI:
10.1016/j.jbiotec.2016.12.023

Journal of Biotechnology 243 (2017) 38–47

Contents lists available at ScienceDirect

Journal of Biotechnology

journal homepage: www.elsevier.com/locate/jbiotec

Characterization of cytochrome P450 CYP109E1 from *Bacillus megaterium* as a novel vitamin D_3 hydroxylase

Ammar Abdulmughni[a], Ilona K. Jóźwik[b], Natalia Putkaradze[a], Elisa Brill[a], Josef Zapp[c], Andy-Mark W.H. Thunnissen[b], Frank Hannemann[a,*], Rita Bernhardt[a,*]

[a] *Department of Biochemistry, Campus B2.2, 66123, Saarland University, Saarbrücken, Germany*
[b] *Laboratory of Biophysical Chemistry, Groningen Biomolecular Sciences and Biotechnology Institute, University of Groningen, Nijenborgh 7, 9747 AG, Groningen, The Netherlands*
[c] *Pharmaceutical Biology, Campus C2.2, 66123, Saarland University, Saarbrücken, Germany*

ARTICLE INFO

Article history:
Received 22 September 2016
Received in revised form
26 December 2016
Accepted 28 December 2016
Available online 30 December 2016

Keywords:
Bacillus megaterium
CYP109E1
Whole-cell conversion
Vitamin D_3
25-Hydroxy-vitamin D_3
Site-directed mutagenesis

ABSTRACT

In this study the ability of CYP109E1 from *Bacillus megaterium* to metabolize vitamin D_3 (VD_3) was investigated. In an *in vitro* system using bovine adrenodoxin reductase (AdR) and adrenodoxin (Adx_{4-108}), VD_3 was converted by CYP109E1 into several products. Furthermore, a whole-cell system in *B. megaterium* MS941 was established. The new system showed a conversion of 95% after 24 h. By NMR analysis it was found that CYP109E1 catalyzes hydroxylation of VD_3 at carbons C-24 and C-25, resulting in the formation of 24(*S*)-hydroxyvitamin D_3 (24S(OH)VD_3), 25-hydroxyvitamin D_3 (25(OH)VD_3) and 24S,25-dihydroxyvitamin D_3 (24S,25$(OH)_2VD_3$). Through time dependent whole-cell conversion of VD_3, we identified that the formation of 24S,25$(OH)_2VD_3$ by CYP109E1 is derived from VD_3 via the intermediate 24S(OH)VD_3. Moreover, using docking analysis and site-directed mutagenesis, we identified important active site residues capable of determining substrate specificity and regio-selectivity. HPLC analysis of the whole-cell conversion with the I85A-mutant revealed an increased selectivity towards 25-hydroxylation of VD_3 compared with the wild type activity, resulting in an approximately 2-fold increase of 25(OH)VD_3 production (45 mg l^{-1} day^{-1}) compared to wild type (24.5 mg l^{-1} day^{-1}).

1. Introduction

Cytochromes P450 (P450s) are heme-containing enzymes found in all domains of life (Nelson, 2011). They are involved in many metabolic processes, including the biosynthesis of steroids and fatty acids, the metabolism of drugs and the detoxification of xenobiotics (Bernhardt, 2006). P450 monooxygenases are gaining importance as enzymes for industrial biotechnology since they have the ability to introduce oxygen into non-activated C—H bonds of various compounds in a regio- and stereo-selective manner under mild conditions (Bernhardt and Urlacher, 2014; Urlacher and Girhard, 2012).

Vitamin D_3 (VD_3) is a fat-soluble prohormone, which is synthesized in the presence of ultraviolet radiation from the precursor 7-dehydrocholestrol (Holick et al., 1979; Kametani and Furuyama, 1987). The activation of VD_3 is achieved by different P450s: the mitochondrial CYP27A1 mediates hydroxylation of VD_3 at carbon 25, producing 25-hydroxyvitamin D_3 (25(OH)VD_3), which is then further hydroxylated by CYP27B1 resulting in the most active form of VD_3, i.e., 1α,25-dihydroxyvitamin D_3 (1α-25$(OH)_2VD_3$) (Prosser and Jones, 2004; Schuster, 2011). It was found that other P450s such as the microsomal CYP2R1, CYP3A4 and CYP2J3 can also hydroxylate VD_3 at C-25 (Cheng et al., 2014; Gupta et al., 2004).

The active form of VD_3, 1α-25$(OH)_2VD_3$, is involved in the regulation of the calcium and phosphate metabolism, amongst other physiological processes (Sakaki et al., 2005; Demay, 2006; Jurutka et al., 2007). However, sufficient levels of the precursor 25(OH)VD_3 are required for the regulatory action of 1α-25$(OH)_2VD_3$ (Di Rosa et al., 2011). Moreover, 25(OH)VD_3 represents the most abundant VD_3 circulating metabolite and, therefore, is used clinically as an indicator for the VD_3 status of patients (Hollis, 2005).

During the last years there has been a growing interest in the biotransformation of VD_3 to its active metabolites, 25(OH)VD_3 and 1α-25$(OH)_2VD_3$. Thereby, recent research activity focused on microbial P450s (Sakaki et al., 2011). However, only few bacterial P450s are known to produce these active metabolites such as CYP105A1 from *S. griseolus* (Sasaki et al., 1991) and CYP107 (Vdh) from *P. autotrophica* (Fujii et al., 2009). Therefore, the identification

* Corresponding authors.
E-mail addresses: f.hannemann@mx.uni-saarland.de (F. Hannemann), ritabern@mx.uni-saarland.de (R. Bernhardt).

http://dx.doi.org/10.1016/j.jbiotec.2016.12.023
0168-1656/

of new microbial P450s with 1-α and/or 25-hydroxylation activity towards VD_3 is of great interest.

Recently, CYP109E1 from *Bacillus megaterium* DSM319 was identified and characterized in our group (Jóźwik et al., 2016). It was shown that CYP109E1 has a 16β-hydroxylation activity towards testosterone. In addition, the X-ray crystal structures of CYP109E1 were solved for substrate-free protein and in complexes with testosterone or corticosterone. In the absence of bound steroids, CYP109E1 contains a large, open active site pocket at the distal side of the heme. The testosterone-bound CYP109E1 structure shows a different conformation, in which the active site pocket is more narrow (closed state of CYP109E1) (Jóźwik et al., 2016), which likely reflects the protein's functionally relevant state and therefore was applied in this study for vitamin D_3 docking calculations.

In this study, the substrate specificity of CYP109E1 was investigated for VD_3. Herein, for the first time we present the results demonstrating that CYP109E1 from *B. megaterium* exhibits hydroxylation activity towards VD_3. In addition, whole-cell conversion of VD_3 was carried out using *B. megaterium*. Furthermore, site-directed mutagenesis based on docking simulations of CYP109E1 and VD_3 was performed in order to optimize the regio-selectivity of CYP109E1 towards 25-hydroxylation. The effect of the mutations on the conversion of VD_3 was examined in the whole-cell system.

2. Materials and methods

2.1. Chemicals

VD_3, 25(OH)VD_3, 1α-25(OH)$_2VD_3$, (2-hydroxypropyl)-β-cyclodextrin and saponin (from quillaja bark) were purchased from Sigma-Aldrich Chemie GmbH (Steinheim, Germnay). Isopropyl β-D-1-thiogalactopyranoside (IPTG) and 5-aminolevulinic acid were purchased from Carbolution chemicals (Saarbruecken, Germany). Bacterial media were purchased from Becton Dickinson (Heidelberg, Germany). All other chemicals were from standard sources and of highest purity available.

2.2. Bacterial strains and plasmids

Cloning experiments were carried out with *E. coli* Top10 (Invitrogen, San Diego, USA). The *E. coli* strain C43 (DE3) for the heterologous protein expressions was purchased from Lucigen Corporation (Wisconsin, USA). Whole-cell conversions were carried out using *B. megaterium* MS941 (Wittchen and Meinhardt, 1995; Stammen et al., 2010). pET17b (Merck Bioscience, Bad Soden, Germnay) and pSMF2.1 (Bleif et al., 2012) were used for expression purposes in *E. coli* and *B. megaterium*, respectively.

2.3. Cloning of CYP109E1

The coding region for CYP109E1 (GenBank GeneID 9119265) was amplified by polymerase chain reaction (PCR) using genomic DNA of *B. megaterium* MS941 as template. The coding region of CYP109E1 was cloned into the *Spe*I and *Kpn*I restriction sites of pSMF2.1, yielding pSMF2.1.CYP109E1. The gene of CYP109E1 with a hexahistidine tag at the C-terminus was cloned into *Nde*I and *Kpn*I restriction sites of pET17b, yielding pET17b.CYP109E1.

2.4. Site-directed mutagenesis

The mutants of CYP109E1 were generated by the QuikChange site-directed mutagenesis method using the plasmid pSMF2.1.CYP109E1 as template and Phusion DNA polymerase (Thermo Fisher Scientific GmbH, Dreireich, Germany). The PCR primers (MWG-Biotech AG, Ebersberg, Germany) were designed to introduce point mutation at the desired positions. The oligonucleotide primers for mutagenesis are shown in Table 1. The reactions were performed in a 50 μl volume using a gradient cycler (PTC-200 DNA Engine cycler). 20 cycles were carried out as follows: initial denaturation at 95 °C for 30 s, denaturation at 95 °C for 30 s, annealing at 58 °C for 30 s and extension at 72 °C for 4 min. Correct generation of the desired mutations was confirmed by DNA sequencing, carried out by Eurofines-MWG (Ebersberg, Germany).

Table 1
Oligonucleotides used in PCR to generate CYP109E1 mutants.

Primer name	oligonucleotides
I85A-for	5′-ACGAGCCTAGCTAATATTGATCCGCCTAAG-3′
I85A-rev	5′-CTTAGGCGGATCAATATTAGCTAGGCTCGT-3′
I168A-for	5′-TCGGATATTGCCGTAGCCGGTCCTTCTAATAACGAACGT-3′
I168A-rev	5′-ACGTTCGTTATTAGAAGGACCGGCTACGGCAATATCCGA-3′
V169A-for	5′-GATATTATCGCAGCCGGTCCTTCTAATAACGAACGT-3′
V169A-rev	5′-ACGTTCGTTATTAGAAGGACCGGCTGCGATAATATC-3′
K187A-for	5′-CTCCAGCAAGAGGCAATGAAAGCAAATGATGAGC-3′
K187A-rev	5′-GCTCATCATTTGCTTTCATTGCCTCTTGCTGGAG-3′
I241A-for	5′-CTATTTTGCTACTGGCTGCTGGAAACGAAACAACCAC-3′
I241A-rev	5′-GTGGTTGTTTCGTTTCCAGCAGCCAGTAGCAAAATAG-3′

2.5. Heterologous expression in E. coli and purification

To express CYP109E1 and its mutants, *E. coli* C43 (DE3) cells were transformed with the corresponding expression plasmids (pET17b.CYP109E1) and cultured overnight in Luria-Bertani (LB) medium containing ampicillin (100 μg ml^{-1}) at 37 °C and 140 rpm. The seed culture was used to inoculate a 200 ml Terrific Broth (TB) medium containing ampicillin 100 μg ml^{-1} (1:100 dilution) in a 2-l baffled flask. The main culture was grown at 37 °C and 140 rpm. When the OD_{600} reached 0.5, the expression was induced with 1 mM IPTG. 0.5 mM delta-aminolevulinic acid served as heme precursor. The cultures were shifted to 30 °C and 120 rpm for 24 h. The *E. coli* cells were harvested by centrifugation at 4500 rpm for 30 min, and the cell pellets were stored at −20 °C until purification. All purification steps were performed at 4 °C. The cell pellets were resuspended in 50 mM potassium phosphate buffer (pH 7.4) containing 300 mM NaCl and 20% glycerol. Phenylmethylsulphonyl fluoride (PMSF) was added to a final concentration of 1 mM and the suspension was sonicated with a T13-sonotrode for 15 min with an amplitude of 12% and consisted of repeated intervals of 15 s pulse and 15 s pause. Cell free extract was obtained by ultracentrifugation at 30,000 rpm for 30 min. The supernatant was applied to an immobilized metal ion affinity chromatography column (TALON, Takara Bio Europe, Saint-Germain-en-Laye, France) that had been equilibrated with 50 mM potassium phosphate buffer (pH 7.4) containing 300 mM NaCl and 20% glycerol. The column was washed with 5 column volumes of 50 mM potassium phosphate buffer (pH 7.4) containing 300 mM NaCl, 20 mM imidazole and 20% glycerol. The tagged protein was eluted with 50 mM potassium phosphate buffer (pH 7.4) containing 300 mM NaCl, 150 mM imidazole and 20% glycerol. The bovine Adx_{4-108} and AdR were expressed and purified as described elsewhere (Sagara et al., 1993; Uhlmann et al., 1994).

2.6. Carbon monoxide (CO) difference spectroscopy

The reduced CO difference spectra of P450 were measured with a double-beam spectrophotometer (UV-2101PC, Shimadzu, Japan). The concentration of P450 was estimated using a molar extinction coefficient of $\varepsilon_{450\text{-}490} = 91\ mM^{-1}\ cm^{-1}$ referred to the method of Omura and Sato (1964).

2.7. In vitro *conversion of VD_3*

A reconstituted *in vitro* system containing CYP109E1 (1 μM), AdR (3 μM), $Adx_{4\text{-}108}$ (20 μM), $MgCl_2$ (1 mM), and a cofactor regenerating system with glucose-6-phosphate (5 mM) and glucose-6-phosphate dehydrogenase (1 U) was used in a final volume of 250 μl in potassium phosphate buffer (20 mM, pH 7.4). The substrate was dissolved in 2-hydroxypropyl-β-cyclodextrin (2.25% w/v) and added to a final concentration of 200 μM. The reaction was started by addition of 0.5 mM NADPH. After 1 h at 30 °C the reaction was stopped and extracted twice with 2 vol of ethyl acetate. The organic phases were combined, evaporated to dryness and prepared for analysis by high-performance liquid chromatography (HPLC).

2.8. Whole-cell conversion of VD_3

The whole-cell conversions were performed in *B. megaterium* MS941. The cells were transformed with the corresponding pSMF2.1.CYP109E1 plasmid using the polyethylene glycol-mediated protoplast transformation method (Barg et al., 2005). The seed culture was prepared with LB medium (10 μg/ml tetracycline). The main culture (50 ml TB medium, 10 μg/ml tetracycline) was inoculated with 500 μl of seed culture (dilution 1:100) in 300 ml baffled flasks and incubated at 37 °C, 140 rpm. The culture was grown to OD_{578} of 0.4 and recombinant gene expression was induced with xylose (5 mg/ml). The culture was grown further at 30 °C for 24 h with shaking at 140 rpm.

For whole-cell conversion experiments, VD_3 was dissolved in 45% 2-hydroxypropyl-β-cyclodextrin and 4% *Quillaja* Saponin as membrane solubilizing agent. After 24 h of protein expression, 2.5 ml of the substrate solution were added to the 50 ml culture. A final substrate concentration of 200 μM was used for all conversion experiments. Afterwards, the conversion was performed for the indicated time at 30 °C and 120 rpm in 300 ml baffled flasks. 500 μl samples of the cultures were taken after defined time periods, extracted and prepared for HPLC analysis.

Large scale whole-cell conversions for purification of VD_3 metabolites were performed in 2 l baffled flasks using 250 ml of main culture. Cultivation of bacteria as well as the whole-cell conversion and extraction were accomplished as mentioned above. After extraction, organic phases were dried using solvent evaporator and stored at −20 °C under protection from UV light until product purification by HPLC.

2.9. High-performance liquid chromatography (HPLC)

The HPLC was carried out on a Jasco system (Pu-980 HPLC pump, AS-950 sampler, UV-975 UV/visible detector, LG-980-02 gradient unit; Jasco, Gross-Umstadt, Germany) equipped with a Nucleodur 100-5 C18 column (125 × 4 mm; Macherey-Nagel, Düren, Germany). The column temperature was adjusted to 40 °C. The samples were dissolved in 200 μl acetonitrile. The flow rate was 1 ml/min with a linear gradient of 60–100% aqueous acetonitrile for 15 min followed by 100% acetonitrile for 15 min. The UV detection of the substrate and products was accomplished at 265 nm. The absorption properties of the products did not differ from the substrate and, therefore, the product formation was calculated from the relative peak area (area%) of the HPLC chromatograms, dividing each respective product peak area by the sum of all peak areas.

2.10. Product purification

Purification of the products was carried out with reversed-phase HPLC using a preparative column VP 250/8 NUCLEODUR 100-5 C18ec (Macherey-Nagel, Düren, Germany). First, the dried extract was dissolved in an acetonitrile/water mixture and filtered through the Rotilabo syringe filters (0.22 μm, Carl Roth GmbH, Karlsruhe, Germany). For purification of product P2, a linear gradient of 80–100% acetonitrile aqueous solution as a mobile phase for 17 min was applied (UV detection: 265 nm; flow rate: 3.5 – 4 ml/min; column temperature: 40 °C). Products P4 and P5 were purified isocratically using a 65% acetonitrile aqueous solution as a mobile phase for 40 min (UV detection: 265 nm; flow rate: 2.5 ml/min; column temperature: 40 °C). Collected product fractions were combined, evaporated to dryness and analyzed by NMR characterization.

2.11. NMR characterization of the metabolites

The NMR spectra were recorded in $CDCl_3$ with a Bruker Avance 500 NMR spectrometer at 298 K. The chemical shifts were relative to $CHCl_3$ at δ 7.26 (^{1}H NMR) and $CDCl_3$ at δ 77.00 (^{13}C NMR) using the standard δ notation in parts per million. The 1D NMR (^{1}H and ^{13}C NMR) and the 2D NMR spectra (gs-HH-COSY and gs-HSQCED) were recorded using the BRUKER pulse program library.

2.12. Molecular docking

Vitamin D_3 (ligand) was docked into the active site of CYP109E1 (receptor) in its closed conformation (PDB: 5L94, CYP109E1-TES) with the use of Autodock Vina 1.1.2 (Trott and Olson, 2010). The testosterone molecule and all waters were removed, and the resulting model was used as a template for the docking experiments. Coordinates for the ligand were taken form an available crystal structure (PDB: 3VRM); six bonds were kept rotatable as confirmed by manual inspection in AutoDockTools 1.5.6. Hydrogens and Gasteiger charges were also added in AutoDockTools 1.5.6. The protein was kept rigid during docking. The simulation cell was limited to a grid box centered at the heme iron with sides adjusted to cover the whole distal heme pocket (x:28 Å, y:34 Å, z:48 Å). Docking simulations were done in triplicate and twenty docking poses were generated for each simulation. The binding poses were analyzed according to lowest binding energies and distances of the target carbon atom (C-25) to the heme iron. Ligand binding residues were identified by analysis done with LigPlot+ (Laskowski and Swindells, 2011) and further visualized with ViewDock tool in UCSF Chimera (Pettersen et al., 2004).

3. Results

3.1. Bioconversion of vitamin D_3 by CYP109E1

CYP109E1 from *B. megaterium* was previously cloned and characterized in our laboratory (Jóźwik et al., 2016). In order to identify new substrates for this enzyme, screening of a focused library consisting of different steroids was carried out. Hereby, VD_3 was identified as new substrate for CYP109E1. In an *in vitro* reconstituted system containing CYP109E1, AdR and $Adx_{4\text{-}108}$, about 90% of 200 μM VD_3 was converted within 1 h into 7 products with the following distribution: 3%, 15%, 8%, 22%, 42%, 5% and 5% of product 1 to product 7 (P1-P7), respectively (Fig. 1A). Over time, it was observed that the increase in the formation of P2 is related to a corresponding decrease of P5. Therefore, we assumed that P5 is converted by CYP109E1 into P2. Through comparison of the retention time (t_R) of the detected products with that of available authentic standards, P1 (t_R = 4.8 min) and P4 (t_R = 11.6 min) were identified as 1α-25$(OH)_2VD_3$ and 25$(OH)VD_3$, respectively (data not shown).

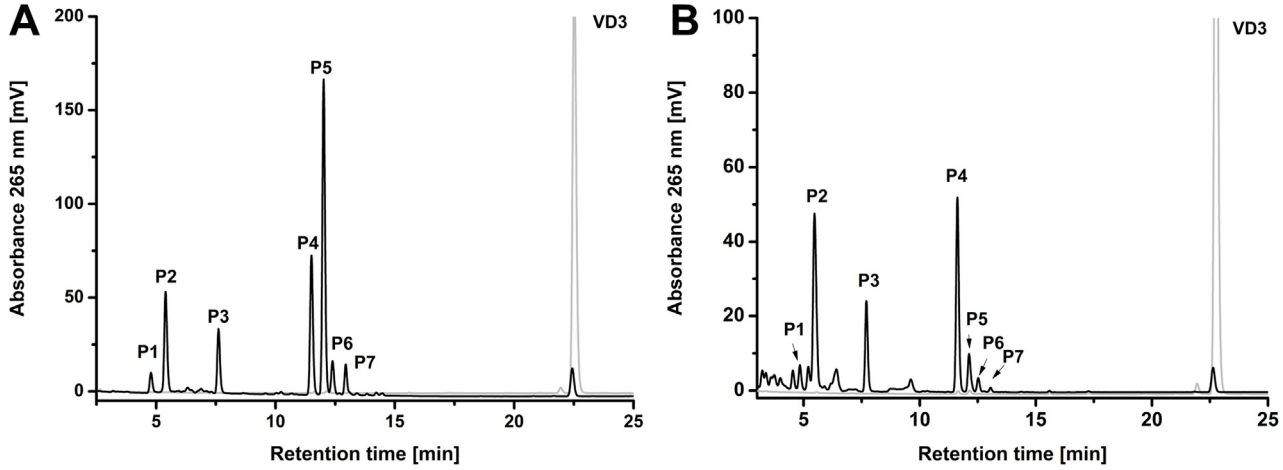

Fig. 1. HPLC chromatogram of the CYP109E1 catalyzed VD_3 conversion. (A) *in vitro* VD_3 conversion, using bovine Adx_{4-108} (20 μM) and AdR (3 μM) and CYP109E1 (1 μM). The reaction was carried out in a final volume of 250 μl at 30 °C for 1 h. (B) CYP109E1-dependent whole-cell conversion of VD_3 in *B. megaterium* MS941. The reaction was carried out in 50 ml TB medium for 24 h at 30 °C. Substrate was added at a final concentration of 200 μM. The peaks of detected products and substrate are labeled with (P1–P7) and VD3, respectively. The authentic standard of 200 μM VD_3 (grey) was detected with the same HPLC method.

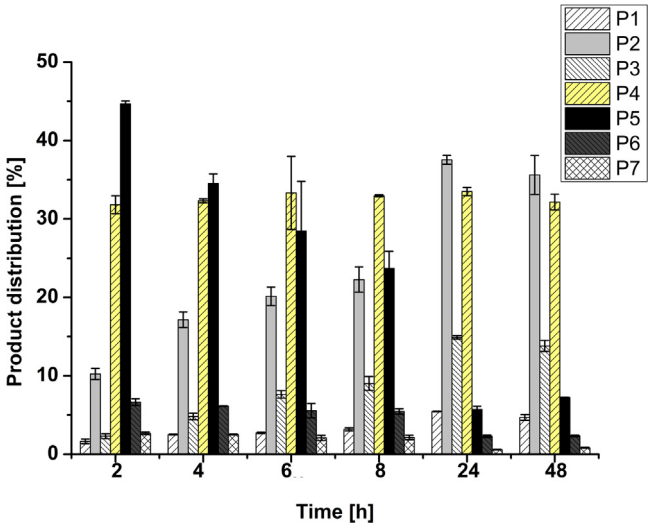

Fig. 2. Product distribution of VD_3 whole-cell conversion in *B. megaterium*. Reactions were carried out in 50 ml TB medium for 48 h at 30 °C. Samples of the cultures were taken after defined time points (2, 4, 6, 8, 24 and 48 h) and analyzed by HPLC as described in "Materials and methods". Labeling of the products (P1–P7) corresponds to that in Fig. 1. The vertical bars indicate the standard deviation values of the mean from two independent experiments.

3.2. *Whole-cell conversion of VD_3 in* B. megaterium

After successful *in vitro* conversion of VD_3, a whole-cell conversion system was established. Fig. 1B shows an HPLC profile of VD_3 whole-cell conversion in *B. megaterium* demonstrating a similar pattern as for the *in vitro* conversion. After 24 h, 95% conversion of 200 μM substrate was achieved (Fig. 2). The product distribution after 24 h conversion was as follows: 6%, 37%, 14%, 33%, 6%, 2% and 2% for products P1-P7, respectively.

For further characterization, we analyzed the time course of product formation during whole-cell conversions, which showed that the product distribution changed over time (Fig. 2). In the first 2 h of the reaction, P5 was found to be the main product with 44% of total share (40 mg l^{-1} day^{-1}). Afterwards, P5 constituted only 5% of total share (4.3 mg l^{-1} day^{-1}). Accompanied by the decrease of P5, an increase of P2 was observed (Fig. 2). The results obtained thus indicate that P2 formation is dependent on the action of CYP109E1 on P5. Therefore, we hypothesized that CYP109E1 has the potency to hydroxylate VD_3 at different positions. To further test, this we decided to identify the main products by nuclear magnetic resonance (NMR) spectroscopy.

3.3. *Large scale conversion of VD_3 and product identification*

In order to obtain sufficient amounts of VD_3 metabolites for further characterization by NMR spectroscopy, whole-cell conversions with a total culture volume of 750 ml were performed. Three products were obtained with sufficient purity and amounts (5–25 mg) for structural characterization via NMR spectroscopy.

In contrast to vitamin D_3, its conversion product P4 showed resonances of an additional tertiary hydroxyl group in the ^{13}C NMR spectrum (δ_C 71.15) and the resonances of the methyl groups C-26 and C-27 appeared both as singlets (δ_H 1.19 s, 6H) in the ^1H NMR spectrum. This cleary indicated hydroxylation at position C-25 and led to the structure of 25(OH)VD_3 for P4. The data were in accordance with those reported in literature (Helmer et al., 1985; Mizhiritskii et al., 1996):

^1H NMR ($CDCl_3$, 500 MHz): δ 0.52 (s, 3xH-18), 0.92 (d, J = 6.5 Hz, 3xH-21), 1.02 (m, H-22a), 1.06 (m, H-22b), 1.19 (s, 6H, 3xH-26 and 3xH-27), 1.20 (m, H-23a), 1.24 (m, H-16a), 1.28 (m, H-17), 1.29 (m, H-12a), 1.36 (m, H-24a), 1.39 (m, H-23b), 1.45 (m, 2H, H-11a and H-24b), 1.51 (m, H-20), 1.52 (m, 2H, H-11b and H-15a), 1.60 (m, H-2a), 1.63 (m, H-15b), 1.69 (m, H-9a), 1.86 (m, H-16b), 1.94 (m, H-14), 1.96 (m, H-2b), 1.98 (m, H-12b), 2.16 (dd, J = 13.5, 8.5 and 5.0 Hz, H-1a), 2.26 (dd, J = 13.0 and 7.5 Hz, H-4a), 2.38 (ddd, J = 13.5, 7.5 and 4.6 Hz, H-1b), 2.55 (dd, J = 13.0 and 4.0 Hz, H-4b), 2.82 (m, H-9b), 3.92 (m, H-3), 4.80 (d, J = 2.5 Hz, H-19a), 5.03 (m, H-19b), 6.01 (d, 11.3 Hz, H-7), 6.21 (d, 11.3 Hz, H-6). ^{13}C NMR ($CDCl_3$, 125 MHz): δ 11.99 (CH_3, C-18), 18.81 (CH_3, C-21), 20.82 (CH_2, C-23), 22.24 (CH_2, C-11), 23.56 (CH_2, C-15), 27.67 (CH_2, C-16), 29.07 (CH_2, C-9), 29.29 (CH_3, C-26), 29.34 (CH_3, C-27), 31.92 (CH_2, C-1), 35.16 (CH_2, C-2), 36.10 (CH_2, C-22), 36.40 (CH, C-20), 40.53 (CH_2, C-12), 44.39 (CH_2, C-24), 45.85 (C, C-13), 45.92 (CH_2, C-4), 56.33 (CH, C-14), 56.53 (CH, C-17), 69.21 (CH, C-3), 71.15 (C, C-25), 112.40 (CH_2, C-19), 117.51 (CH, C-7), 122.45 (CH, C-6), 135.00 (C, C-5), 142.89 (C, C-8), 145.09 (C, C-10).

The NMR spectra of P5 revealed an additional secondary hydroxyl group (δ_H 3.34 m, δ_C 77.41 CH). Its position at C-24 was obvious by vicinal correlations of its proton to the isopropyl proton H-25 (δ_H 1.69 m) in the HHCOSY and to the methyls C-26 (16.69,

CH_3) and C-27 18.93, CH_3) in the HMBC. Comparison of the data with those of an authentic sample (Xi et al., 2014) supported these findings. Especially the chemical shifts of C-1 to C-19 fitted perfectly to each other, whereas the resonances for the side chain slightly differed. This might originate from a different sterochemistry at C-24 in our sample and its epimer from literature. Unfortunately the authors gave no hint to the stereochemistry at C-24 and our sample decomposed within one day in solution. Therefore, the assignment of the absolute configuration at C-24 could not be solved by subsequent NMR measurements, such as Mosherís method. But as was found for closely related 24-hydroxylated steroids the 24(*R*)- and 24(*S*)-isomers showed characteristic differences in the ^{13}C NMR (Koizumi et al., 1979). Applying these observations to our problem led to the identification of the 24(*S*)-form for our molecule and to the 24(*R*)-form for the epimer reported by Xi et al. (2014):

NMR ($CDCl_3$, 500 MHz): δ 0.57 (s, 3xH-18), 0.92 (d, J = 6.9 Hz, 3xH-26), 0.95 (d, J = 6.9 Hz, 3xH-27), 0.97 (d, J = 6.5 Hz, 3xH-21), 1.08 (m, H-22a), 1.28 (m, H-23a), 1.33 (m, H-16a and H-17), 1.34 (m, H-12a), 1.43 (m, H-20), 1.51 (m, H-11a), 1.56 (m, H-15a), 1.58 (m, H-23b), 1.59 (m, H-11b), 1.64 (m, H-22b), 1.68 (m, H-2a), 1.69 (m, H-25), 1.70 (m, H-15b), 1.72 (m, H-9a), 1.93 (m, H-16b), 1.96 (m, H-2b), 2.01 (m, H-14), 2.03 (m, H-12b), 2.20 (dd, J = 13.5, 8.5 and 5.0 Hz, H-1a), 2.30 (dd, J = 13.0 and 7.5 Hz, H-4a), 2.42 (ddd, J = 13.5, 7.8 and 4.6 Hz, H-1b), 2.60 (dd, J = 13.0 and 4.0 Hz, H-4b), 2.86 (m, H-9b), 3.34 (m, H-24), 3.97 (m, H-3), 4.86 (d, J = 2.5 Hz, H-19a), 5.07 (dt, J = 2.5 and 1.3 Hz, H-19b), 6.06 (d, 11.3 Hz, H-7), 6.26 (d, 11.3 Hz, H-6). ^{13}C NMR ($CDCl_3$, 125 MHz): δ 12.00 (CH_3, C-18), 16.69 (CH_3, C-26), 18.93 (CH_3, C-27), 19.05 (CH_3, C-21), 22.23 (CH_2, C-11), 23.55 (CH_2, C-15), 27.62 (CH_2, C-16), 28.99 (CH_2, C-9), 30.74 (CH_2, C-23), 31.91 (CH_2, C-1), 32.16 (CH_2, C-22), 33.15 (CH, C-25), 35.14 (CH_2, C-2), 36.29 (CH, C-20), 40.50 (CH_2, C-12), 45.84 (C, C-13), 45.90 (CH_2, C-4), 56.30 (CH, C-14), 56.37 (CH, C-17), 69.20 (CH, C-3), 77.41 (CH, C-24), 112.44 (CH_2, C-19), 117.51 (CH, C-7), 122.43 (CH, C-6), 135.07 (C, C-5), 142.21 (C, C-8), 145.05 (C, C-10).

P2 was found to be a dihydroxylated conversion product of vitamin D_3. The NMR spectra revealed resonances for a supplementary secondary (δ_C 79.55 CH) and a tertiary (δ_C 73.15C) hydroxyl function. 2D NMR HHCOSY, HSQCED and HMBC measurements revealed their positions as immediate neighbours at C-24 and C-25. According to P5, C-24 in P2 was expected to be in (*S*)-configuration. However, we wanted to prove this assumption in an independent manner. Both epimers were known from literature but no comparative NMR studies were available. Therefore, we performed a comparison of the NMR data of their synthetic precursors, the 24(*R*)- and 24(*S*)-forms of de-A,B-cholesta-8,24,25-triol (Pérez Sestelo et al., 2002). Analysis of the ^{13}C NMR data for the side chain of P2 and comparison with those of the C-24 epimeric de-A,B-cholestanes gave a clear and unambiguous evidence for 24S,25(OH)$_2$VD$_3$ as structure for P2:

NMR ($CDCl_3$, 500 MHz): δ 0.55 (s, 3xH-18), 0.95 (d, J = 6.5 Hz, 3xH-21), 1.04 (m, H-22a), 1.14 (m, H-23a), 1.17 (s, 3xH-26), 1.22 (s, 3xH-27), 1.28 (m, H-17), 1.29 (m, H-16a), 1.31 (m, H-12a), 1.41 (m, H-20), 1.49 (m, 2H, H-11a and H-11b), 1.54 (m, H-15a), 1.57 (m, H-23b), 1.68 (m, H-2a and H-15b), 1.69 (m, H-9a), 1.77 (m, H-22b), 1.89 (m, H-16b), 1.94 (m, H-2b), 1.98 (m, H-14), 2.00 (m, H-12b), 2.21 (m, H-1a), 2.30 (dd, J = 13.0 and 7.5 Hz, H-4a), 2.41 (ddd, J = 13.5, 7.8 and 4.6 Hz, H-1b), 2.58 (dd, J = 13.0 and 4.0 Hz, H-4b), 2.83 (m, H-9b), 3.29 (d, J = 10.1 and 2.0 Hz, H-24), 3.94 (m, H-3), 5.05 (dt, J = 2.5 and 1.3 Hz, H-19b), 4.82 (d, J = 2.5 Hz, H-19a), 6.03 (d, 11.3 Hz, H-7), 6.23 (d, 11.3 Hz, H-6). ^{13}C NMR ($CDCl_3$, 125 MHz): δ 12.00 (CH_3, C-18), 18.94 (CH_3, C-21), 22.23 (CH_2, C-11), 23.17 (CH_3, C-26), 23.54 (CH_2, C-15), 26.51 (CH_3, C-27), 27.61 (CH_2, C-16), 28.34 (CH_2, C-23), 28.99 (CH_2, C-9), 31.95 (CH_2, C-1), 33.22 (CH_2, C-22), 35.19 (CH_2, C-2), 36.26 (CH, C-20), 40.51 (CH_2, C-12), 45.83 (C, C-13), 45.94 (CH_2, C-4), 56.28 (CH, C-14), 56.39 (CH, C-17), 69.20 (CH, C-3), 73.17 (C, C-25), 79.55 (CH, C-24), 112.42 (CH_2, C-19), 117.56 (CH, C-7), 122.33 (CH, C-6), 135.21 (C, C-5), 142.08 (C, C-8), 145.09 (C, C-10).

These results confirmed our assumption, that CYP109E1 can hydroxylate VD_3 at different positions. As shown above, the ratio of P2 (24S,25(OH)$_2$VD$_3$) increased inversely proportional to the ratio of P5 (24S(OH)VD$_3$) over time, indicating that CYP109E1 has 25-hydroxylation activity towards VD_3 as well as 24S(OH)VD$_3$. The reaction pathway of VD_3 conversion by CYP109E1 is shown in Fig. 3.

3.4. Molecular docking of VD_3 to CYP109E1

Unfortunately soaking/co-crystallization trials to obtain the structure of the CYP109E1-VD_3 complex proved unsuccessful, therefore docking of the VD_3 molecule was performed to identify potential substrate-binding residues. A structural comparison of CYP109E1 to other P450s converting VD_3 found in the PDB, revealed that the closed conformer of CYP109E1 (PDB: 5L94) is highly similar to the closed state observed for CYP107 (Vdh) crystallized in com plex with VD_3 (PDB: 3A50, Yasutake et al., 2010, r.m.s.d of 1.23 Å for 347 Cα atoms). Therefore, the closed conformation of CYP109E1 likely reflects the functionally relevant conformational state of the protein and was chosen in this study for the substrate docking calculations. Among the calculated VD_3 conformations, the one showing a suitable distance of the C-25 atom to the heme iron and the lowest predicted free energy of binding was chosen for further analysis. The docked pose places the aliphatic side chain of VD_3 close to the heme iron, productively for 25-hydroxylation (C-25-Fe distance of 3.7 Å), and is well in agreement with the crystallographically observed VD_3 binding mode in CYP107 (Vdh) (C-25-Fe distance of 4.6 Å). The only hydrophilic group (3β-OH group at the A-ring) of VD_3 is solvent exposed, predicted not to interact with any of the protein side chains; the rest of the VD_3 molecule interacts with hydrophobic residues lining the active site pocket, similarly as in Vdh. Since VD_3 hydroxylation is of outstanding importance for sustainable biotransformation process of the production of active VD_3, we were interested to improve the yield of 25(OH)VD$_3$. Four amino acids predicted to interact with VD_3 were mutated to alanine to determine their roles in CYP109E1 activity and selectivity towards VD_3: I85 (BC-loop, substrate recognition site 1, SRS1), I168 and V69 (F-helix, SRS2) and I241 (I-helix, SRS4) Additionally, one more residue was chosen for mutagenesis, K187 (SRS3), since its mutation to alanine in CYP109E1 was previously shown to cause a slight decrease in testosterone conversion activity. Thus we considered the possibility that this flexible residue, located at the top of the active site (G helix), might also take part in VD_3 binding (Fig. 4).

3.5. Conversion of VD_3 by CYP109E1 mutants

To investigate the effect of selected mutations on activity and regio-selectivity of CYP109E1 towards VD_3 directly in the whole-cell system, *B. megaterium* cells were transformed with the plasmid pSMF2.1.CYP109E1 containing the corresponding CYP109E1 mutations. The results clearly showed that all CYP109E1 mutants still maintained VD_3 hydroxylation activity. However, activity or/and selectivity of CYP109E1 was affected by the amino acid replacements (Fig. 5).

While the K187A mutant showed the same conversion ratio (97%) as compared with wild type, the activity of CYP109E1 was changed by selected mutations (Fig. 6). All other mutants showed decreased activity in the first 8 h of the reaction. However, the activity in case of I85A, I168A, V169A and I241A mutants was increased afterwards. After 24 h conversion, the I168A mutant exhibited a comparable conversion (96%) as the wild type and the I85A mutant showed a maximum conversion of 87%. On the other hand, a significant decrease of the activity was observed in case of V169A and

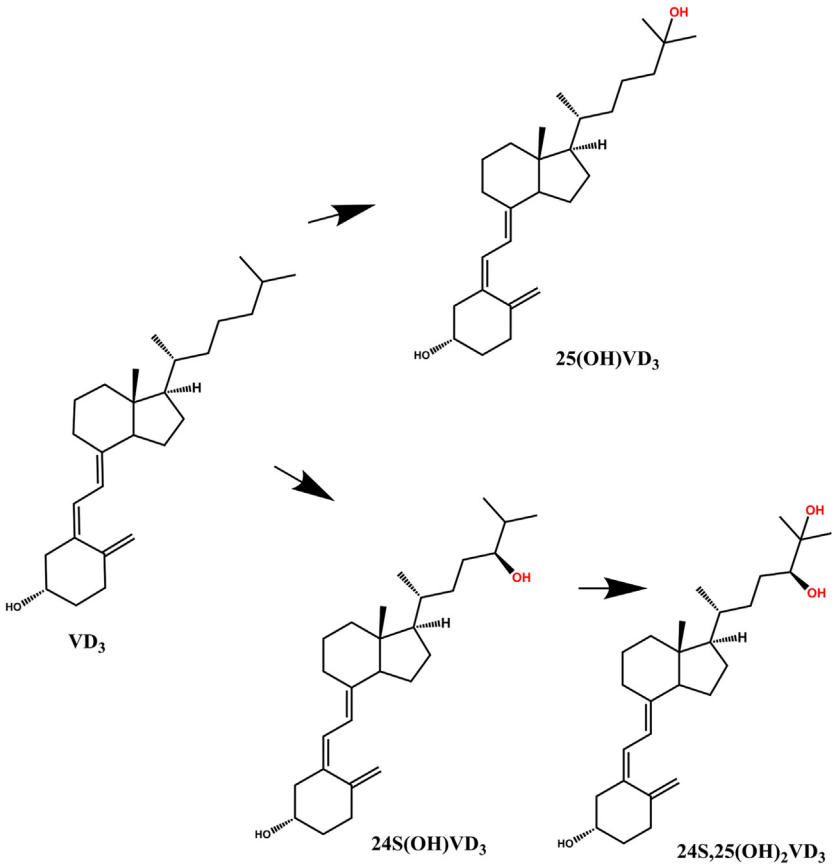

Fig. 3. Reaction pathway of VD_3 by CYP109E1 from *B. megaterium*.

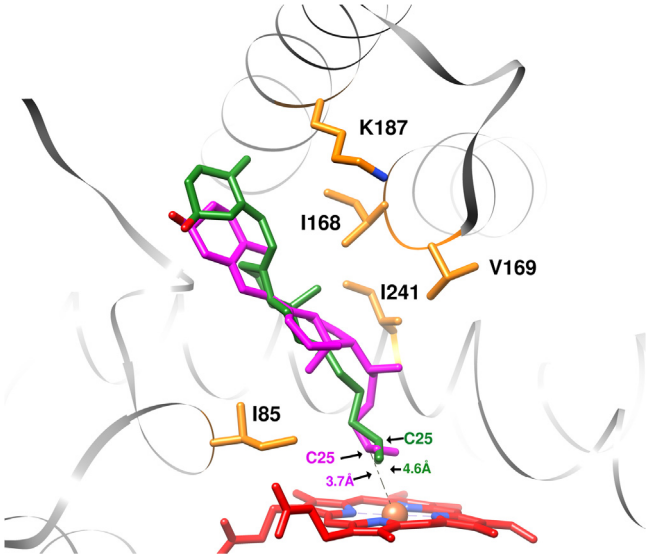

Fig. 4. Docking model of VD_3 in the active site of CYP109E1. The suitable conformation of VD_3 for 25-hydroxylation is shown (in *magenta*), and compared to the crystallographically observed VD_3 binding mode in CYP107 (Vdh) (in *green*). Heme is in *red* coloured sticks. Amino acids selected for site-directed mutagenesis are shown in *orange* sticks. (For interpretation of the references to color in this figure legend, the reader is referred to the web version of this article.)

I241A mutants, displaying only 76% and 54% conversion, respectively.

Additionally, the effect of the point mutations on the regio-selectivity of CYP109E1-dependent VD_3 conversion was studied (Table 2). Compared to wild type, the formation of 24S(OH)VD_3 was decreased over time in case of the I85A and I168A mutants, which, as a consequence, led to reduced amounts of the derived product 24S,25$(OH)_2VD_3$. On the other hand, the 25-hydroxylation activity towards VD_3 was strongly preferred in the reactions catalyzed by the I85A and I168A mutants resulting in 63% and 49% of total products, respectively (Table 2). Moreover, mutant I85A displayed a significant reduction in the number of products Consequently, an increase of the absolute 25(OH)VD_3 production was observed with these mutants, compared to the wild type (Fig. 7). These results indicate that the side chains of amino acids I85 and I168 are essential for determining the regio-selectivity of CYP109E1 towards VD_3. Compared to wild type, the regio-selectivity of the K187A mutant was also slightly changed towards 25-hydroxylation (Table 2). Furthermore, it was observed that the 24S,25$(OH)_2VD_3$ production decreased in the whole-cell conversion with the K187A mutant, compared to wild type. In contrast to the decrease in the 24S,25$(OH)_2VD_3$ production, an accumulation of 24S(OH)VD_3 was observed, suggesting that the K187A mutant has less specificity towards 24S(OH)VD_3, compared to wild type.

Furthermore, significant changes of the specificity and regio-selectivity of CYP109E1 were determined in whole-cell conversions with the V169A and I241A mutants. Compared to the wild type, it was observed that reactions of variant V169A showed a decreased 25-hydroxylation activity of 24S(OH)VD_3, whereas the 25-hydroxylation of VD_3 was enhanced (Table 2). In addition, no formation of P1, P3 and P7 was observed with this mutant. In whole-cell conversions with the V169A mutant, the product distribution was as follows: 24S(OH)VD_3 (40%), 25(OH)VD_3 (47%), 24S,25$(OH)_2VD_3$ (3%) and P6 (10%). It was further observed that the substitution of I241 to alanine shifts the regio-selectivity of CYP109E1 towards 24-hydroxylation (60% of total products). In

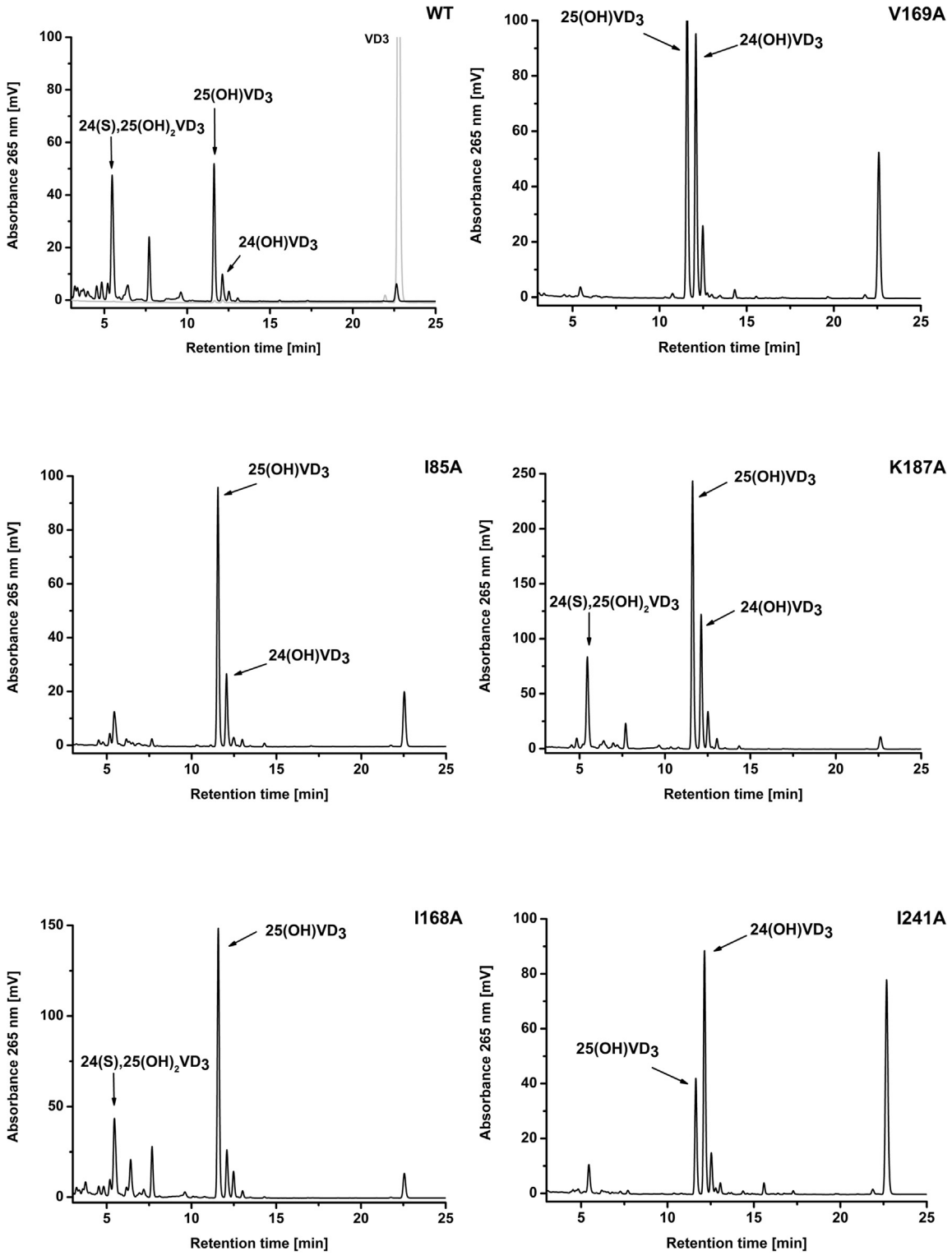

Fig. 5. HPLC chromatograms of VD_3 whole-cell conversions by *B. megaterium* expressing different variants of CYP109E1. The reactions were carried out in 50 ml TB medium for 24 h at 30 °C. The substrate was added at a final concentration of 200 μM. The authentic standard of 200 μM VD_3 (grey) was detected with the same HPLC method.

contrast, a decrease of 24S,25 $(OH)_2VD_3$ was observed (only 3% of total products) indicating that the 25-hydroxylation activity of this mutant of CYP109E1 towards 24S$(OH)VD_3$ is dramatically decreased.

4. Discussion

During the past years bioconversion processes, including specific hydroxylations, have gained increasing interest, since chemical synthesis often requires complex procedures and environmentally unfriendly conditions. The ability of P450s to

Table 2
Comparison of products distribution of 24 h whole-cell conversions of VD_3 by different variants of CYP109E1.

Enzyme variant	Conversion [%]	Number of products	Major product(s) [%][a]
Wild type	95	7	24S,25(OH)$_2$VD$_3$ (37%) 25(OH)VD$_3$ (33%)
I85A	87.3	3	25(OH)VD$_3$ (63%)
I168A	94	7	24S,25(OH)$_2$VD$_3$ (20%) 25(OH)VD$_3$ (49%)
V169A	75.4	3	25(OH)VD$_3$ (47%) 24S(OH)VD$_3$ (42%)
K187A	96.8	7	25(OH)VD$_3$ (45%) 24S(OH)VD$_3$ (22%)
I241A	53.8	4	25(OH)VD$_3$ (27%) 24S(OH)VD$_3$ (58%)

[a] Only products with a ratio of ≥20% of total products are defined here as major products.

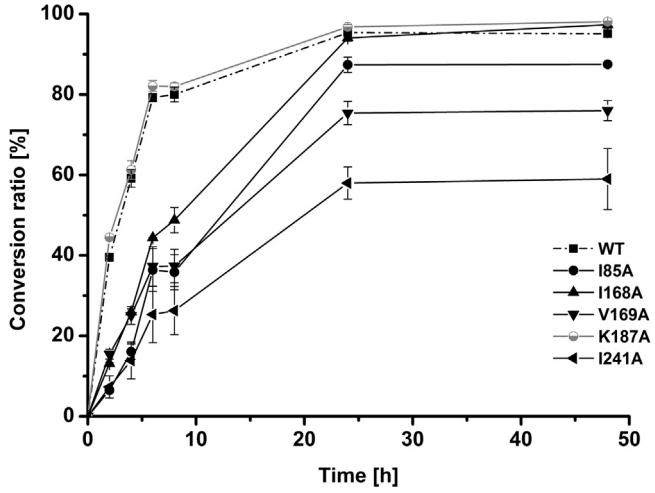

Fig. 6. Effect of selected mutations in CYP109E1 on the conversion of VD_3. Reactions were performed using *B. megaterium* MS941 in 50 ml TB medium at 30 °C. The substrate was added at a final concentration of 200 μM. Samples of the cultures were taken after defined time points (2, 4, 6, 8, 24 and 48 h) and analyzed by HPLC as described in "Materials and methods". The vertical bars indicate the standard deviation values of the mean from three independent whole-cell experiments.

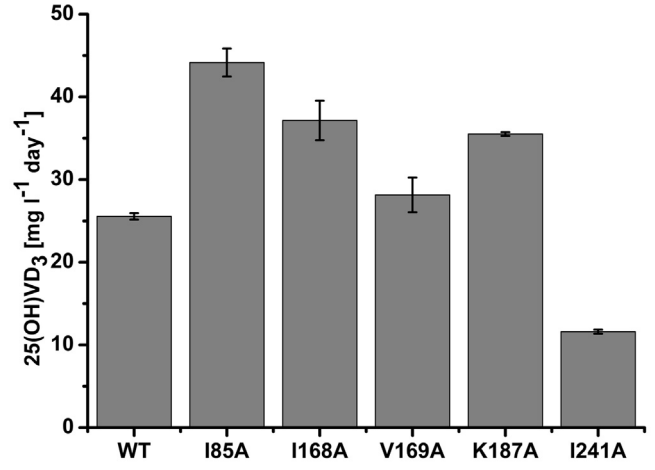

Fig. 7. Production of 25(OH)VD_3 in *B. megaterium* overexpressing different variants of CYP109E1. Reactions were performed in 50 ml TB medium for 24 h at 30 °C. The substrate was added at a final concentration of 200 μM. The amount of 25(OH)VD_3 was measured by HPLC as described in "Materials and methods". The vertical bars indicate the standard deviation values of the mean from three independent whole-cell experiments.

hydroxylate a broad range of compounds makes them suitable as versatile biocatalysts (Bernhardt, 2006; Bernhardt and Urlacher, 2014).

It is known that VD_3 is activated in kidneys and liver by different P450s such as mitochondrial cytochromes CYP27A1 and CYP27B1 as well as the microsomal enzymes CYP2R1, CYP3A4 and CYP2J3. However, low activity and stability of mammalian P450s compared with those of bacterial origin are important factors limiting their industrial applications (Julsing et al., 2008). As a result of such limitation, bacterial P450s constitute an attractive alternative for the industrial production of different valuable products, including VD_3 metabolites. Until now, only a few studies have reported the usage of bacterial P450s for the production of VD_3 metabolites such as CYP105A1 and CYP107 (Vdh) (Sakaki et al., 2011). Therefore, the identification of new bacterial P450s with hydroxylation activity towards VD_3 is of a great interest for the industry. In particular, *B. megaterium* offers a great potential, both as a source and expression host, for such new bacterial P450s. It has been used since many decades for the production of different industrial enzymes (Vary et al., 2007; Korneli et al., 2013). It offers an advantage that replicative plasmids are stable and maintained (Stammen et al., 2010). In addition, *B. megaterium* lacks external alkaline proteases and, therefore, is suitable for heterologous protein expression. Moreover, *B. megaterium* can grow on simple media utilizing a broad spectrum of carbon sources (Vary, 1994).

Therefore, the establishment of *B. megaterium*-based whole cell system using a bacterial P450 as biocatalyst for the production of active VD_3 metabolites, such as 25(OH)VD_3, is an interesting alternative for the industrial production. Recently, *B. megaterium* was used in our laboratory for the conversion of the steroid hormone precursor cholesterol to pregnenolone and for the hydroxylation of 11-keto-β-boswellic acid (KBA) (Gerber et al., 2015; Bleif et al., 2012; Brill et al., 2014). Moreover, a CYP27A1-based whole-cell system was established in *B. megaterium* allowing efficient production of valuable pharmaceuticals such as 27-hydroxycholesterol, 26/27-hydroxy-7-dehydrocholesterol, 25(OH)VD_3 and 25-hydroxy-7-dehydrocholesterol (Ehrhardt et al., 2016).

In this study, we demonstrated for the first time the conversion of VD_3 by a member of the CYP109 family, namely CYP109E1 from *B. megaterium* DSM319. We showed that CYP109E1 can convert VD_3 into different products, in both enzyme-based and whole-cell-based assays. The new whole-cell system converts more than 90% of the added substrate (200 μM) within 24 h supporting its promising potential as VD_3 hydroxylase. The two main products of CYP109E1-dependent conversion of VD_3 were identified by NMR analysis as 25(OH)VD_3 (33%) and 24S, 25 (OH)$_2$$VD_3$ (37%) with yields of 24.5 mg l^{-1} day^{-1} and 28.6 mg l^{-1} day^{-1}, respectively. In addition, the product P5 was identified by NMR analysis as 24S(OH)VD_3. For further characterization of product formation, time-dependent whole-cell conversions were performed. It was

shown that both, 24S(OH)VD_3 (P5) and 25(OH)VD_3 (P4), are initially detected as major products (Fig. 3). Nevertheless, a decrease in the 24S(OH)VD_3 ratio was observed in correlation with the formation of 24S,25$(OH)_2VD_3$ (P2). In contrast, the ratio of 25(OH)VD_3 was relatively constant over time (30–33% of total products). Thus we conclude that the formation of 24S,25$(OH)_2VD_3$ from VD_3 proceeds via the intermediate 24S(OH)VD_3. This is to the best of our knowledge a novel reaction pathway of VD_3 leading to 24S,25$(OH)_2VD_3$ via 24S(OH)VD_3. In addition, these results demonstrate that CYP109E1 has a 25-hydroxylation activity towards VD_3 as well as 24S(OH)VD_3.

It is known that the hydroxylation of VD_3 at C-25 is the first step of the VD_3 activation (Prosser and Jones, 2004; Sakaki et al., 2005; Schuster, 2011). 25(OH)VD_3 is the best indicator of the nutritional status of VD_3 in the circulation (Hollis, 2005). This compound has been gaining importance in recent years as it was shown to be a better therapeutic agent for several diseases than VD_3 itself, due to its direct biological effect and better intestinal absorption (Jean et al., 2008; Leichtmann et al., 1991). It was found that supplementation of 25(OH)VD_3 has a preventive, therapeutic effect against diseases such as hyperglycemia, chronic kidney disease, Crohn's and cholestatic liver disease (Jean et al., 2008; Leichtmann et al., 1991). In addition to applications of this metabolite for human health, it is used as supplement in animal feed (Soares et al., 1995). Whereas specific biological activities for the natural VD_3 metabolite 24R,25$(OH)_2VD_3$ were identified (Norman et al., 1983; St-Arnaud and Glorieux, 1998; Yamato et al., 1989), so far no functions are known for its unnatural epimer 24S,25$(OH)_2VD_3$, which was identified here in the CYP109E1-based whole cell conversion of VD_3.

Our aim in the next step of this study was the enhancement of the 25(OH)VD_3 production yield by CYP109E1. Since the crystal structure of a VD_3-bound CYP109E1 complex is not available, the putative substrate-binding residues were predicted with docking simulations. It is anticipated that VD_3 binds with its aliphatic side chain close to the heme iron and the C-25 atom is in a suitable distance for hydroxylation (Fig. 4). High similarity of the CYP109E1-VD_3 model with the experimental CYP107 (Vdh)-VD_3 crystal structure gives credence to the reliability of our docking results. A similar set of hydrophobic residues is predicted to interact with VD_3 in CYP109E1, including I85, I241, I168 and V169, which correspond to I88, I235, L171, and V172 in Vdh (Yasutake et al., 2010). To test their potential role in VD_3 binding and conversion in CYP109E1, these four residues were targeted for mutation to alanines. In addition, residue K187 was chosen for mutagenesis, to test whether this flexible residue may play a role in substrate binding by interacting with the 3β-OH group of VD_3. Previously, it was shown that mutation of this residue to an alanine slightly lowers the conversion rate of testosterone by CYP109E1 (Jóźwik et al., 2016). However, our results show that considering VD_3 hydroxylation, the mutation of K187 to alanine does not influence CYP109E1 activity (Fig. 6). Thus, residue K187 plays no role in VD3 binding by CYP109E1, in accordance with the docking results and with the lack of substrate binding interactions by the equivalent residue (K180) in the VD_3-bound crystal structure of Vdh.

Mutagenesis of the other four residues (I85, I168, V169 and I241) ultimately yielded an improved regio-selectivity of CYP109E1 towards VD_3. It has been found that all mutants, except I241A, exhibited a higher selectivity towards 25-hydroxylation than the wild type (Table 2). This enhancement of the regio-selectivity resulted in an increase of the 25(OH)VD_3 production upon whole-cell conversion of VD_3 (Fig. 7). Compared to the wild type, approximately a 2-fold increase of the 25(OH)VD_3 yield was achieved with the I85A mutant, 45 mg l^{-1} day^{-1} compared to 24.5 mg l^{-1} day^{-1}. In the literature, the conversion yield of 25(OH)VD_3 by the most widely investigated P450 for vitamin D_3 hydroxylation, CYP105A1, had been initially very low and was later significantly improved by protein engineering (Sasaki et al., 1991). The most productive mutant of CYP105A1 (R73A/R84A) is reported to produce 8.3 mg l^{-1} day^{-1} of 25(OH)VD_3 (Hayashi et al., 2010; Sakaki et al., 2011). Residue I85 of CYP109E1, as mentioned above, is located in SRS1, in the close vicinity of the heme, and is one of the most investigated residues in P450s. The corresponding position in different P450s was described to interact with the P450s ligands and, therefore, to affect the activity and selectivity of the enzyme (Gricman et al., 2015). The importance of this position was observed in case of CYP102A1 as the substitutions of F87 caused improved selectivity towards propylbenzene and terpene substrates, among others (Gricman et al., 2015; Li et al., 2001; Seifert et al., 2009). In addition, the substitution of S122 to threonine in CYP1A1 (corresponding position to I85 in CYP109E1 and F87 in CYP102A1) improved the 7-methoxy- and 7-ethoxyresorufin O-dealkylase activity (Liu et al., 2004).

Furthermore, our results showed that the substitution of V169 or I241 to alanine residues significantly diminished the conversion of the 24S(OH)VD_3 intermediate into 24S,25$(OH)_2VD_3$, as compared to reactions with the wild type enzyme. The functional importance of V169 and I241 was also previously determined for testosterone conversion by CYP109E1 (Jóźwik et al., 2016). It was shown that by substituting either residue to an alanine the activity of CYP109E1 towards testosterone is completely abolished. Therefore, we suggest that V169 and I241 of CYP109E1 are substrate specificity-determining residues.

5. Conclusions

This study describes the identification of a new VD_3 hydroxylase from *B. megaterium*, CYP109E1, with 25- and 24-hydroxylation activity. The established *B. megaterium*-based whole-cell system for the conversion of VD_3 has a promising potential for the biotechnological production of the valuable metabolite 25(OH)VD_3.

In addition, further investigations on CYP109E1 were performed in order to increase the production of 25(OH)VD_3. Based on docking studies, site-directed mutagenesis was performed at selected positions in the active site of the enzyme. We were able to demonstrate the importance of selected active site residues for VD_3 conversion. A change of the regio-selectivity and substrate specificity was observed for most of the mutants. A considerable increase of the production of the valuable metabolite 25(OH)VD_3 was achieved with the I85A mutant. In addition, two novel metabolites of VD_3, 24S(OH)VD_3 and 24S,25$(OH)_2VD_3$, have been identified, whose potential for further drug development needs to be investigated.

Competing interests

The authors declare that they have no competing interest.

Author contributions

AA designed and carried out the experiments, analyzed and interpreted the results and drafted the manuscript. IJ performed the docking simulations and assisted in drafting the manuscript. NP and EB purified the products for NMR analysis. EB carried out the substrate screening. JZ performed the NMR measurements and structure determination of vitamin D_3 metabolites. AT analyzed and interpreted the results, and assisted in drafting the manuscript. FH and RB designed the project, analyzed and interpreted the results, and assisted in drafting the manuscript. All authors read and approved the final manuscript.

Acknowledgments

This work was kindly supported by the German Federation of Industrial Research Associations (AIF/ZIM project FKZ 2214512AJA). The authors would like to thank Birgit Heider-Lips for the purification of AdR and Adx_{4-108}. Thanks to Mohammed Milhim for proof reading.

References

Barg, H., Malten, M., Jahn, M., Jahn, D., 2005. Protein and vitamin production in*Bacillus megaterium*. In: Barredo, J.-L. (Ed.), Microbial Processes and Products, Methods in Biotechnology. Humana Press, pp. 205–223.

Bernhardt, R., Urlacher, V.B., 2014. Cytochromes P450 as promising catalysts for biotechnological application: chances and limitations. Appl. Microbiol. Biotechnol. 98, 6185–6203.

Bernhardt, R., 2006. Cytochromes P450 as versatile biocatalysts. J. Biotechnol. 124, 128–145.

Bleif, S., Hannemann, F., Zapp, J., Hartmann, D., Jauch, J., Bernhardt, R., 2012. A new *Bacillus megaterium* whole-cell catalyst for the hydroxylation of the pentacyclic triterpene 11-keto-β-boswellic acid (KBA) based on a recombinant cytochrome P450 system. Appl. Microbiol. Biotechnol. 93, 1135–1146.

Brill, E., Hannemann, F., Zapp, J., Brüning, G., Jauch, J., Bernhardt, R., 2014. A new cytochrome P450 system from *Bacillus megaterium* DSM319 for the hydroxylation of 11-keto-β-boswellic acid (KBA). Appl. Microbiol. Biotechnol. 98, 1701–1717.

Cheng, C.Y.S., Slominski, A.T., Tuckey, R.C., 2014. Metabolism of 20-hydroxyvitamin D3 by mouse liver microsomes. J. Steroid Biochem. Mol. Biol. 144 (Part B), 286–293.

Demay, M.B., 2006. Mechanism of vitamin D receptor action. Ann. N. Y. Acad. Sci. 1068, 204–213.

Di Rosa, M., Malaguarnera, M., Nicoletti, F., Malaguarnera, L., 2011. Vitamin D3: a helpful immuno-modulator. Immunology 134, 123–139.

Ehrhardt, M., Gerber, A., Hannemann, F., Bernhardt, R., 2016. Expression of human CYP27A1 in *B. megaterium* for the efficient hydroxylation of cholesterol, vitamin D3 and 7-dehydrocholesterol. J. Biotechnol. 218, 34–40.

Fujii, Y., Kabumoto, H., Nishimura, K., Fujii, T., Yanai, S., Takeda, K., Tamura, N., Arisawa, A., Tamura, T., 2009. Purification, characterization, and directed evolution study of a vitamin D3 hydroxylase from Pseudonocardia autotrophica. Biochem. Biophys. Res. Commun. 385, 170–175.

Gerber, A., Kleser, M., Biedendieck, R., Bernhardt, R., Hannemann, F., 2015. Functionalized PHB granules provide the basis for the efficient side-chain cleavage of cholesterol and analogs in recombinant Bacillus megaterium. Microb. Cell Factories 14.

Gricman, Ł., Vogel, C., Pleiss, J., 2015. Identification of universal selectivity-determining positions in cytochrome P450 monooxygenases by systematic sequence-based literature mining. Proteins Struct. Funct. Bioinf. 83, 1593–1603.

Gupta, R.P., Hollis, B.W., Patel, S.B., Patrick, K.S., Bell, N.H., 2004. CYP3A4 is a human microsomal vitamin D 25-hydroxylase. J. Bone Miner. Res. 19, 680–688.

Hayashi, K., Yasuda, K., Sugimoto, H., Ikushiro, S., Kamakura, M., Kittaka, A., Horst, R.L., Chen, T.C., Ohta, M., Shiro, Y., Sakaki, T., 2010. Three-step hydroxylation of vitamin D3 by a genetically engineered CYP105A1. FEBS J. 277, 3999–4009.

Helmer, B., Schnoes, H.K., DeLuca, H.F., 1985. 1H nuclear magnetic resonance studies of the conformations of vitamin D compounds in various solvents. Arch. Biochem. Biophys. 241, 608–615.

Holick, M.F., Richtand, N.M., McNeill, S.C., Holick, S.A., Frommer, J.E., Henley, J.W., Potts, J.T., 1979. Isolation and identification of previtamin D3 from the skin of rats exposed to ultraviolet irradiation. Biochemistry (Mosc.) 18, 1003–1008.

Hollis, B.W., 2005. Circulating 25-hydroxyvitamin D levels indicative of vitamin D sufficiency: implications for establishing a new effective dietary intake recommendation for vitamin D. J. Nutr. 135, 317–322.

Jóźwik, I.K., Kiss, F.M., Gricman, Ł., Abdulmughni, A., Brill, E., Zapp, J., Pleiss, J., Bernhardt, R., Thunnissen, A.-M.W.H., 2016. Structural basis of steroid binding and oxidation by the cytochrome P450 CYP109E1 from*Bacillus megaterium*. FEBS J. 283, 4128–4148.

Jean, G., Terrat, J.-C., Vanel, T., Hurot, J.-M., Lorriaux, C., Mayor, B., Chazot, C., 2008. Daily oral 25-hydroxycholecalciferol supplementation for vitamin D deficiency in haemodialysis patients: effects on mineral metabolism and bone markers. Nephrol. Dial. Transplant. 23, 3670–3676.

Julsing, M.K., Cornelissen, S., Bühler, B., Schmid, A., 2008. Heme-iron oxygenases: powerful industrial biocatalysts? Curr. Opin. Chem. Biol. 12, 177–186.

Jurutka, P.W., Bartik, L., Whitfield, G.K., Mathern, D.R., Barthel, T.K., Gurevich, M., Hsieh, J.-C., Kaczmarska, M., Haussler, C.A., Haussler, M.R., 2007. Vitamin D receptor: key roles in bone mineral pathophysiology, molecular mechanism of action, and novel nutritional ligands. J. Bone Miner. Res. Off. J. Am. Soc. Bone Miner. Res. 22 (Suppl. 2), V2–10.

Kametani, T., Furuyama, H., 1987. Synthesis of vitamin D3 and related compounds. Med. Res. Rev. 7, 147–171.

Koizumi, N., Fujimoto, Y., Takeshita, T., Ikekawa, N., 1979. Carbon-13 nuclear magnetic resonance of 24-substituted steroids. Chem. Pharm. Bull. (Tokyo) 27, 38–42.

Korneli, C., David, F., Biedendieck, R., Jahn, D., Wittmann, C., 2013. Getting the big beast to work—systems biotechnology of *Bacillusmegaterium* for novel high-value proteins. J. Biotechnol. 163, 87–96.

Laskowski, R.A., Swindells, M.B., 2011. LigPlot+: multiple ligand-protein interaction diagrams for drug discovery. J. Chem. Inf. Model. 51, 2778–2786.

Leichtmann, G.A., Bengoa, J.M., Bolt, M.J., Sitrin, M.D., 1991. Intestinal absorption of cholecalciferol and 25-hydroxycholecalciferol in patients with both Crohn's disease and intestinal resection. Am. J. Clin. Nutr. 54, 548–552.

Li, Q.S., Ogawa, J., Schmid, R.D., Shimizu, S., 2001. Residue size at position 87 of cytochrome P450 BM-3 determines its stereoselectivity in propylbenzene and 3-chlorostyrene oxidation. FEBS Lett. 508, 249–252.

Liu, J., Ericksen, S.S., Sivaneri, M., Besspiata, D., Fisher, C.W., Szklarz, G.D., 2004. The effect of reciprocal active site mutations in human cytochromes P450 1A1 and 1A2 on alkoxyresorufin metabolism. Arch. Biochem. Biophys. 424, 33–43.

Mizhiritskii, M.D., Konstantinovskii, L.E., Vishkautsan, R., 1996. 2D NMR study of solution conformations and complete 1H and 13C chemical shifts assignments of vitamin D metabolites and analogs. Tetrahedron 52, 1239–1252.

Nelson, D.R., 2011. Progress in tracing the evolutionary paths of cytochrome P450. Biochim. Biophys. Acta 1814, 14–18, Proteins Proteomics, Cytochrome P450: Structure, biodiversity and potential for application.

Norman, A.W., Leathers, V., Bishop, J.E., 1983. Normal egg hatchability requires the simultaneous administration to the hen of 1 alpha, 25-dihydroxycholecalciferol and 24R,25-dihydroxycholecalciferol. J. Nutr. 113, 2505–2515.

Omura, T., Sato, R., 1964. The carbon monoxide-binding pigment of liver microsomes. J. Biol. Chem. 239, 2370–2378.

Pérez Sestelo, J., Cornella, I., de Uña, O., Mouriño, A., Sarandeses, L.A., 2002. Stereoselective convergent synthesis of 24,25-dihydroxyvitamin D3 metabolites: a practical approach. Chem. Weinh. Bergstr. Ger. 8, 2747–2752.

Pettersen, E.F., Goddard, T.D., Huang, C.C., Couch, G.S., Greenblatt, D.M., Meng, E.C., Ferrin, T.E., 2004. UCSF Chimera–a visualization system for exploratory research and analysis. J. Comput. Chem. 25, 1605–1612.

Prosser, D.E., Jones, G., 2004. Enzymes involved in the activation and inactivation of vitamin D. Trends Biochem. Sci. 29, 664–673.

Sagara, Y., Wada, A., Takata, Y., Waterman, M.R., Sekimizu, K., Horiuchi, T., 1993. Direct expression of adrenodoxin reductase in *Escherichia coli* and the functional characterization. Biol. Pharm. Bull. 16, 627–630.

Sakaki, T., Kagawa, N., Yamamoto, K., Inouye, K., 2005. Metabolism of vitamin D3 by cytochromes P450. Front. Biosci. J. Virtual Lib. 10, 119–134.

Sakaki, T., Sugimoto, H., Hayashi, K., Yasuda, K., Munetsuna, E., Kamakura, M., Ikushiro, S., Shiro, Y., 2011. Bioconversion of vitamin D to its active form by bacterial or mammalian cytochrome P450. Biochim. Biophys. Acta BBA – Proteins Proteom. 1814, 249–256.

Sasaki, J., Mikami, A., Mizoue, K., Omura, S., 1991. Transformation of 25- and 1 alpha-hydroxyvitamin D3 to 1 alpha: 25-dihydroxyvitamin D3 by using *Streptomyces* sp. strains. Appl. Environ. Microbiol. 57, 2841–2846.

Schuster, I., 2011. Cytochromes P450 are essential players in the vitamin D signaling system. Biochim. Biophys. Acta 1814, 186–199.

Seifert, A., Vomund, S., Grohmann, K., Kriening, S., Urlacher, V.B., Laschat, S., Pleiss, J., 2009. Rational design of a minimal and highly enriched CYP102A1 mutant library with improved regio-, stereo- and chemoselectivity. Chembiochem. Eur. J. Chem. Biol. 10, 853–861.

Soares, J.H., Kerr, J.M., Gray, R.W., 1995. 25-hydroxycholecalciferol in poultry nutrition. Poult. Sci. 74, 1919–1934.

St-Arnaud, R., Glorieux, F.H., 1998. Editorial: 24, 25-dihydroxyvitamin D—active metabolite or inactive catabolite? Endocrinology 139, 3371–3374.

Stammen, S., Müller, B.K., Korneli, C., Biedendieck, R., Gamer, M., Franco-Lara, E., Jahn, D., 2010. High-yield intra- and extracellular protein production using *Bacillus megaterium*. Appl. Environ. Microbiol. 76, 4037–4046.

Trott, O., Olson, A.J., 2010. AutoDock Vina: improving the speed and accuracy of docking with a new scoring function, efficient optimization, and multithreading. J. Comput. Chem. 31, 455–461.

Uhlmann, H., Kraft, R., Bernhardt, R., 1994. C-terminal region of adrenodoxin affects its structural integrity and determines differences in its electron transfer function to cytochrome P-450. J. Biol. Chem. 269, 22557–22564.

Urlacher, V.B., Girhard, M., 2012. Cytochrome P450 monooxygenases: an update on perspectives for synthetic application. Trends Biotechnol. 30, 26–36.

Vary, P.S., Biedendieck, R., Fuerch, T., Meinhardt, F., Rohde, M., Deckwer, W.-D., Jahn, D., 2007. *Bacillus megaterium*—from simple soil bacterium to industrial protein production host. Appl. Microbiol. Biotechnol. 76, 957–967.

Vary, P.S., 1994. Prime time for *Bacillus megaterium*. Microbiol. Read. Engl. 140 (Pt. 5), 1001–1013.

Wittchen, K.D., Meinhardt, F., 1995. Inactivation of the major extracellular protease from *Bacillus megaterium* DSM319 by gene replacement. Appl. Microbiol. Biotechnol. 42, 871–877.

Xi, Z., Zhai, L., Xie, H., Zeng, Z., 2014. Preparation and identification of the related impurities from biotransformed calcifediol. Jingxi-Huagong 31, 979–982.

Yamato, H., Matsumoto, T., Fukumoto, S., Ikeda, K., Ishizuka, S., Ogata, E., 1989. Effect of 24,25-dihydroxyvitamin D3 on 1,25-dihydroxyvitamin D3 [1,25-(OH)2D3] metabolism in vitamin D-deficient rats infused with 1,25-(OH)2D3. Endocrinology 124, 511–517.

Yasutake, Y., Fujii, Y., Nishioka, T., Cheon, W.-K., Arisawa, A., Tamura, T., 2010. Structural evidence for enhancement of sequential vitamin D3 hydroxylation activities by directed evolution of cytochrome P450 vitamin D3 hydroxylase. J. Biol. Chem. 285, 31193–31201.